ANALYSIS OF THE SUITABILITY OF LUMPED FORMULATIONS FOR ADSORBED NATURAL GAS STORAGE

D. S. Jurumenha, diegojurumenha@hotmail.com[1]
L. A. Sphaier, lasphaier@mec.uff.br[1]

[1]Laboratório de Mecânica Teórica e Aplicada, Programa de Pós-Graduação em Engenharia Mecânica, Departamento de Engenharia Mecânica, Universidade Federal Fluminense, Rua Passo da Pátria 156, bloco E, sala 216, Niterói, RJ, 24210-240, Brazil

Abstract: Adsorbed gas storage has been demonstrated to be an interesting alternative to the currently adopted storages modes. However, the thermal effects inherent to the sorption phenomena tend to reduce gas storage and recovery capabilities. This effect can be minimized if an effective thermal design is conducted. In this context, computational simulations can be of great assistance. Nevertheless, the complexities associated with modeling the heat and mass transfer that occur within adsorbed gas processes can lead to formulations that require a great computational effort. This paper shows that a complex multidimensional formulation can be reduced to a simple lumped formulation via an averaging procedure. Naturally, this simpler formulation cannot represent accurately a significant number of cases. Hence, a comparison between the simpler lumped formulation with a one that considers spatial dependence is provided, showing the range of applicability of the simpler form.

Keywords: Natural gas; Methane; Adsorption; Heat and mass transfer; Lumped Analysis

1. NOMENCLATURE

Bi	Biot number	t	time
c_p	constant pressure specific heat	T	temperature
C^*	thermal capacity ratio	$\mathcal{V}$	reservoir volume
Fo	Fourier number	**Greek Symbols**	
i	specific enthalpy	ρ	specific mass
i_{sor}	heat of sorption	ϵ	porosity
j	mass flux coponent	σ	Darcy equation coefficient
k	thermal conductivity	**Subscripts**	
H^*	dimensionless heat transfer coefficient	e	effective or apparent
m	mass	g	gas phase
$\dot{m}$	mass flow rate	i	inter-particle voids
M_l^*	adsorbed fraction	l	adsorbed (liquid) phase
p	pressure	s	solid phase
q	heat flux component	w	reservoir wall
R^*	thermal resistance ratio	T	isothermal operation
u	specific internal energy		

2. INTRODUCTION

When looking into the current widely adopted natural gas storage modes, namely Compressed Natural Gas (CNG) and Liquified Natural Gas (LNG), two clear disadvantages associated with each of these modes are seen. Compressed gas, has the disadvantage of working with high pressures (generally around 25 MPa), which naturally require heavy reservoirs. On the other hand, liquified gas require cryogenic temperatures and special as well as specialized equipment for re-gasification. In this scenario, Adsorbed Natural Gas (ANG) becomes an attractive option, since it has none of the previously mentioned problems. Nevertheless, the adsorption process is exothermic, and the resulting heating effect can significantly diminish storage capacity. A cooling effect also occurs during desorption, reducing the amount of gas that can be recovered during discharge. In spite of the inherent problem associated with the thermal effects of adsorption, the undesired heating and cooling can be greatly minimized if an adequate design is proposed. Naturally, this would

require a proper understanding of the transport phenomena involved during charge and discharge operations. Because of this, a number of mathematical models have been proposed to simulate the mechanics of adsorbed natural gas. The works of Barbosa Mota *et al.* (1997a,b) provided a formulation for evaluating charge and discharge dynamics of adsorbed methane. In (Vasiliev *et al.*, 2000), the authors employed a model that takes into account temperature variations in radial and axial directions, but gas concentration variations were considered only in the radial direction. Bastos-Neto *et al.* (2005) considered a model similar to the one used in (Barbosa Mota *et al.*, 1997b); however, no intra-particle diffusion effects were considered. Another similar heat and mass transfer model was employed by Basumatary *et al.* (2005); however, in that study, the thermal conductivity of the adsorbent medium was allowed to vary with temperature. Different from the above mentioned studies, Walton and LeVan (2006) presented a one-dimensional mathematical model for examining the influence of non-isothermal effects and impurities contained in natural gas during storage-cycles, and Zhou (1997) employed a simple lumped formulation for natural gas storage. Recently, Hirata *et al.* (2009) presented a one-dimensional model for gas discharge and employed a hybrid analytical-numerical methodology for the solution of the governing equations. A one-dimensional formulation was also employed by Santos *et al.* (2009). Very recently, a new lumped formulation was proposed in da Silva and Sphaier (2010).

Working with complex mathematical formulations unavoidably leads to a harder computational effort for simulating transport phenomena. As a result, one always seeks simplifications to the equations. Probably one one the most used simplifications is that of lumped-capacitance formulations, in which gradients in one (or more) directions are assumed small, thereby reducing the number of spatial dimensions needed to characterize the problem. Nevertheless, for using lumped formulations one needs to ensure that the small gradient conditions are actually met for a given physical problem. For simple decoupled heat diffusion problems without heat generation, this is usually given by the magnitude of a single parameter – the Biot number; however in more complex situations, a single parameter is not enough. This paper presents an analysis for determining the suitability of lumped formulations for the coupled heat and mass transfer that occur during the discharge of ANG reservoirs.

3. MATHEMATICAL FORMULATION

The problem of mono-component ideal gas storage in reservoir filled with adsorbent material can be described by different formulations (Barbosa Mota *et al.*, 1997a,b; Vasiliev *et al.*, 2000; Bastos-Neto *et al.*, 2005; Hirata *et al.*, 2009); however, when usual simplifying assumptions such as ideal gas behavior and no intra-particle diffusion effects are considered, a common formulation is obtained. By introducing the dimensionless groups developed in (Sacsa Diaz and Sphaier, 2010), the following normalized version of the problem arises:

$$\mathrm{M}_g^* \frac{\partial \rho_g^*}{\partial t^*} + \mathrm{M}_l^* \frac{\partial \rho_l^*}{\partial t^*} = -\nabla^* \cdot \boldsymbol{j}_g^*, \tag{1}$$

$$\left(\mathrm{M}_g^* \rho_g^* + c_p^* \mathrm{M}_l^* \rho_l^* + \mathrm{C}^*\right) \frac{\partial T^*}{\partial t^*} + \boldsymbol{j}_g^* \cdot (\nabla^* T^*) = -\mathrm{Fo}^+ \nabla^* \cdot \boldsymbol{q}^* + \mathrm{M}_l^* i_{sor}^* \frac{\partial \rho_l^*}{\partial t^*} + \mathrm{M}_g^* \omega \frac{\partial p^*}{\partial t^*} \tag{2}$$

where C^* is the added contribution of the thermal capacity ratios

$$\mathrm{C}^* = \mathrm{C}_s^* + \mathrm{C}_{\min}^*. \tag{3}$$

The dimensionless boundary conditions are given by, at $\mathcal{S}_i$ (inlet/outlet surface)[1]:

$$\boldsymbol{j}_g^* \cdot \hat{\boldsymbol{n}} = j_{in}^*, \tag{4}$$

$$\boldsymbol{q}^* \cdot \hat{\boldsymbol{n}} = -k_e^* (\nabla^* T^*) \cdot \hat{\boldsymbol{n}} = \mathrm{Bi}_{in}^+ (T^* - T_{io}^*). \tag{5}$$

and at $\mathcal{S}_e$ (remaining surface):

$$\boldsymbol{j}_g^* \cdot \hat{\boldsymbol{n}} = 0, \tag{6}$$

$$\boldsymbol{q}^* \cdot \hat{\boldsymbol{n}} = -k_e^* (\nabla^* T^*) \cdot \hat{\boldsymbol{n}} = \mathrm{Bi} (T^* - 1) + \frac{1}{\mathrm{Fo}_w R^*} \frac{\partial T^*}{\partial t^*}, \tag{7}$$

The initial conditions are given by

$$p^*(t^* = 0) = p_0^*, \qquad T^*(t^* = 0) = 1, \tag{8}$$

in which $p_0^* = 1$ for discharge and $p_0^* = 0$ for charge.

---

[1] where the situation of prescribed mass influx (or outflux) is considered.

3.1 Dimensionless groups

The first dimensionless groupings represent the fractions of gas that are stored in gaseous form and in adsorbed form, being defined as

$$\mathrm{M}_g^* = \frac{\Delta \rho_g \, \epsilon \, \mathcal{V}}{\Delta m_{\max}}, \qquad \mathrm{M}_l^* = \frac{\Delta \rho_l \, \mathcal{V}}{\Delta m_{\max}}, \qquad \text{where} \qquad \Delta m_{\max} = (\Delta \rho_g \, \epsilon + \Delta \rho_l) \, \mathcal{V}. \tag{9}$$

and the $\Delta \rho$ differences are given by:

$$\Delta \rho_g = \rho_{g,\max} - \rho_{g,\min}, \qquad \Delta \rho_l = \rho_{l,\max} - \rho_{l,\min}, \tag{10}$$

The next parameters comprise thermal capacity ratios between different capacities and the thermal capacity of the amount of gas charged (or discharged) under isothermal conditions. In this context, the thermal capacity ratios of the adsorbent material, the reservoir wall and the minimum gas contained in the reservoir are respectively defined as:

$$\mathrm{C}_s^* = \frac{c_s \, \rho_b \, \mathcal{V}}{c_{p_g} \, \Delta m_{\max}}, \qquad \mathrm{C}_w^* = \frac{c_w \, m_w}{c_{p_g} \, \Delta m_{\max}}, \tag{11}$$

$$\mathrm{C}_{\min}^* = \frac{\left(\epsilon \, c_{p_g} \, \rho_{g,\min} + c_l \, \rho_{l,\min} \right) \mathcal{V}}{c_{p_g} \, \Delta m_{\max}}. \tag{12}$$

The Fourier number for the bed is defined as

$$\mathrm{Fo} = \frac{\alpha_b \, t_f}{L^2}, \qquad \text{with} \qquad \alpha_b = \frac{k_b}{\rho_b \, c_s}, \tag{13}$$

where k_b is the bed conductivity. A modified Fourier number is also defined:

$$\mathrm{Fo}^+ = \mathrm{C}_s^* \, \mathrm{Fo} = \frac{\alpha_b^+ \, t_f}{L^2}, \qquad \text{with} \qquad \alpha_b^+ = \frac{k_b \, \mathcal{V}}{\Delta m_{\max} \, c_{p_g}}. \tag{14}$$

Biot numbers are given by

$$\mathrm{Bi} = \frac{h \, L}{k_b}, \qquad \mathrm{Bi}_{in} = \frac{h_{in} \, L}{k_b}, \qquad \mathrm{Bi}_{in}^+ = \mathrm{Bi}_{in} + j_{in}^* / \mathrm{Fo}^+. \tag{15}$$

The dimensionless heat of sorption and the ratio between specific heats of gaseous and adsorbed phases are defined as:

$$c_p^* = \frac{c_l}{c_{p_g}}, \qquad i_{sor}^* = \frac{i_{sor}}{T_0 \, c_{p_g}}. \tag{16}$$

Another parameter related to the gas behavior is the thermodynamic ratio ω, which is reduced to the following expression for ideal gases:

$$\omega = \frac{R}{c_{p_g}} = \frac{\kappa - 1}{\kappa}, \qquad \text{where} \qquad \kappa = c_{p_g} / c_{v_g}. \tag{17}$$

3.2 Dimensionless variables

The dependent and independent variables are normalized by introducing the following dimensionless forms:

$$t^* = \frac{t}{t_f}, \qquad T^* = \frac{T}{T_0}, \qquad p^* = \frac{p - p_{\min}}{\Delta p}, \tag{18}$$

$$\rho_g^* = \frac{\rho_g - \rho_{g,\min}}{\Delta \rho_g}, \qquad \rho_l^* = \frac{\rho_l - \rho_{l,\min}}{\Delta \rho_l}. \tag{19}$$

where $\Delta p = p_{\max} - p_{\min}$.

The dimensionless nabla operator is defined as:

$$\nabla^* = L \, \nabla \tag{20}$$

And the dimensionless mass flux vector is given by:

$$\boldsymbol{j}^* = \frac{\boldsymbol{j}'' \, t_f}{\Delta m_{\max} \, L / \mathcal{V}}, \tag{21}$$

such that dimensionless versions for the inlet mass flux, the mass inflow rate, and the total mass stored in the reservoir are obtained:

$$j_{in}^* = \frac{\dot{m}_{in}'' \, t_f}{\Delta m_{\max} \, L/\mathcal{V}}, \qquad \dot{m}_{in}^* = \frac{\dot{m}_{in} \, t_f}{\Delta m_{\max}}, \qquad m^* = \frac{m_{\mathrm{real}}}{\Delta m_{\max}}. \tag{22}$$

With the dimensionless variables, the dimensionless mass flux in the gas phase can be written as:

$$\boldsymbol{j}_g^* = -\mathrm{M}_g^* \, (\rho_g^* + \rho_{g,\min}^*) \, \sigma^* \, \nabla^* p^*, \qquad \text{where} \qquad \sigma^* = \sigma \, \frac{\Delta p \, t_f}{L^2}, \qquad \rho_{g,\min}^* = \frac{\rho_{g,\min}}{\Delta \rho_g}. \tag{23}$$

Finally, the heat conduction vector is also written as a dimensionless flux:

$$\boldsymbol{q}^* = -k_e^* \, \nabla^* T^*, \qquad \text{with} \qquad k_e^* = \frac{k_e}{k_b}. \tag{24}$$

4. LUMPING PROCEDURE

Before beginning the lumping procedure, a space-average quantity is defined:

$$\bar{\phi} = \frac{1}{\mathcal{V}^*} \int_{\mathcal{V}^*} \phi \, \mathrm{d}\mathcal{V}^* \tag{25}$$

The lumping of the differential formulation given by equations (1) and (2) consists of integrating these equations within the reservoir volume, $\mathcal{V}^*$ (in dimensionless form). However, it is first convenient to write the energy equation in in conservative form:

$$\frac{\partial}{\partial t^*} \left(T^* \left(\mathrm{M}_g^* \, \rho_g^* + c_p^* \, \mathrm{M}_l^* \, \rho_l^* + \mathrm{C}^* \right) \right) + (1 - c_p^*) \, \mathrm{M}_l^* \, \frac{\partial \rho_l^*}{\partial t^*} \, T^* + \nabla^* \cdot (\boldsymbol{j}_g^* \, T^*) =$$
$$= -\mathrm{Fo}^+ \, \nabla^* \cdot \boldsymbol{q}^* + \mathrm{M}_l^* \, i_{sor}^* \, \frac{\partial \rho_l^*}{\partial t^*} + \mathrm{M}_g^* \, \omega \, \frac{\partial p^*}{\partial t^*} \tag{26}$$

Then, the energy and mass conservation equations are volume-integrated, leading to:

$$\left(\mathrm{M}_g^* \, \frac{\mathrm{d}\bar{\rho}_g^*}{\mathrm{d}t^*} + \mathrm{M}_l^* \, \frac{\partial \bar{\rho}_l^*}{\partial t^*} \right) \mathcal{V}^* = - \int_{\mathcal{S}^*} \boldsymbol{j}_g^* \cdot \hat{\boldsymbol{n}} \, \mathrm{d}\mathcal{A}^*, \tag{27}$$

$$\frac{\mathrm{d}}{\mathrm{d}t^*} \int_{\mathcal{V}^*} \left(T^* \left(\mathrm{M}_g^* \, \rho_g^* + c_p^* \, \mathrm{M}_l^* \, \rho_l^* + \mathrm{C}^* \right) \right) \mathrm{d}\mathcal{V}^* + (1 - c_p^*) \, \mathrm{M}_l^* \int_{\mathcal{V}^*} \frac{\partial \rho_l^*}{\partial t^*} \, T^* \, \mathrm{d}\mathcal{V}^* + \int_{\mathcal{S}^*} (\boldsymbol{j}_g^* \, T^*) \cdot \hat{\boldsymbol{n}} \, \mathrm{d}\mathcal{A}^* =$$
$$= -\mathrm{Fo}^+ \int_{\mathcal{S}^*} \boldsymbol{q}^* \cdot \hat{\boldsymbol{n}} \, \mathrm{d}\mathcal{A}^* + \left(\mathrm{M}_l^* \, i_{sor}^* \, \frac{\mathrm{d}\bar{\rho}_l^*}{\mathrm{d}t^*} + \mathrm{M}_g^* \, \omega \, \frac{\mathrm{d}\bar{p}^*}{\mathrm{d}t^*} \right) \mathcal{V}^* \tag{28}$$

As usually considered for natural gas, $c_p^* = 1$ is assumed, such that the integrated energy equation is simplified:

$$\frac{\mathrm{d}}{\mathrm{d}t^*} \int_{\mathcal{V}^*} \left(T^* \left(\mathrm{M}_g^* \, \rho_g^* + \mathrm{M}_l^* \, \rho_l^* + \mathrm{C}^* \right) \right) \mathrm{d}\mathcal{V}^* + \int_{\mathcal{S}^*} (\boldsymbol{j}_g^* \, T^*) \cdot \hat{\boldsymbol{n}} \, \mathrm{d}\mathcal{A}^* =$$
$$= -\mathrm{Fo}^+ \int_{\mathcal{S}^*} \boldsymbol{q}^* \cdot \hat{\boldsymbol{n}} \, \mathrm{d}\mathcal{A}^* + \left(\mathrm{M}_l^* \, i_{sor}^* \, \frac{\mathrm{d}\bar{\rho}_l^*}{\mathrm{d}t^*} + \mathrm{M}_g^* \, \omega \, \frac{\mathrm{d}\bar{p}^*}{\mathrm{d}t^*} \right) \mathcal{V}^* \tag{29}$$

Then, by introducing the boundary conditions, the surface integrals involving the heat and mass fluxes are given by:

$$\int_{\mathcal{S}^*} \boldsymbol{j}_g^* \cdot \hat{\boldsymbol{n}} \, \mathrm{d}\mathcal{A}^* = -j_{in}^* \, \mathcal{A}_i^* \tag{30}$$

$$\int_{\mathcal{S}^*} \boldsymbol{q}^* \cdot \hat{\boldsymbol{n}} \, \mathrm{d}\mathcal{A}^* = \mathrm{Bi}_{in}^+ \left(T^*|_{\mathcal{A}_i^*} - T_{io}^* \right) \mathcal{A}_i^* + \mathrm{Bi} \left(T^*|_{\mathcal{A}_e^*} - 1 \right) \mathcal{A}_e^* + \frac{1}{\mathrm{Fo}_w \, R^*} \frac{\partial T^*|_{\mathcal{A}_e^*}}{\partial t^*} \, \mathcal{A}_e^* \tag{31}$$

$$\int_{\mathcal{S}^*} (\boldsymbol{j}_g^* \, T^*) \cdot \hat{\boldsymbol{n}} \, \mathrm{d}\mathcal{A}^* = -j_{in}^* \, T^*|_{\mathcal{A}_i^*} \, \mathcal{A}_i^* \tag{32}$$

Substituting the surface integrals into the space-integrated equations gives:

$$\left(\mathrm{M}_g^* \, \frac{\mathrm{d}\bar{\rho}_g^*}{\mathrm{d}t^*} + \mathrm{M}_l^* \, \frac{\partial \bar{\rho}_l^*}{\partial t^*} \right) \mathcal{V}^* = j_{in}^* \, \mathcal{A}_i^*, \tag{33}$$

$$\frac{\mathrm{d}}{\mathrm{d}t^*} \int_{\mathcal{V}^*} \left(T^* \left(\mathrm{M}_g^* \, \rho_g^* + \mathrm{M}_l^* \, \rho_l^* + \mathrm{C}^* \right) \right) \mathrm{d}\mathcal{V}^* - j_{in}^* \, T^*|_{\mathcal{A}_i^*} \, \mathcal{A}_i^* = - \frac{\mathrm{Fo}^+}{\mathrm{Fo}_w \, R^*} \frac{\partial T^*|_{\mathcal{A}_e^*}}{\partial t^*} \, \mathcal{A}_e^* +$$

$$- \mathrm{Fo}^+ \left(\mathrm{Bi} \left(T^*|_{\mathcal{A}_e^*} - 1 \right) \mathcal{A}_e^* + \mathrm{Bi}_{in}^+ \left(T^*|_{\mathcal{A}_i^*} - T_{io}^* \right) \mathcal{A}_i^* \right) + \left(\mathrm{M}_l^* \, i_{sor}^* \, \frac{\mathrm{d}\bar{\rho}_l^*}{\mathrm{d}t^*} + \mathrm{M}_g^* \, \omega \, \frac{\mathrm{d}\bar{p}^*}{\mathrm{d}t^*} \right) \mathcal{V}^* \quad (34)$$

The mass conservation equation above is already in the final lumped form, an needs no further work. The energy equation requires some more manipulation. One then considers the classical lumped approximation:

$$T^*|_{\mathcal{A}_i^*} \approx T^*|_{\mathcal{A}_e^*} \approx \bar{T}^* \tag{35}$$

However, this approximation cannot be applied to the advective term, which must be treated separately. Two different situations must be considered, as described below:

$$\int_{\mathcal{S}^*} (\boldsymbol{j}_g^* \, T^*) \cdot \hat{\boldsymbol{n}} \, \mathrm{d}\mathcal{A}^* = -j_{in}^* \, T^*|_{\mathcal{A}_i^*} \, \mathcal{A}_i^* \approx -j_{in}^* \, T_{io}^* \, \mathcal{A}_i^*, \qquad \text{for charge} \tag{36}$$

$$\int_{\mathcal{S}^*} (\boldsymbol{j}_g^* \, T^*) \cdot \hat{\boldsymbol{n}} \, \mathrm{d}\mathcal{A}^* = -j_{in}^* \, T^*|_{\mathcal{A}_i^*} \, \mathcal{A}_i^* \approx -j_{in}^* \, \bar{T}^* \, \mathcal{A}_i^*, \qquad \text{for discharge} \tag{37}$$

Considering a discharge operation, the energy equation is then rearranged as:

$$\left(\mathrm{M}_g^* \, \bar{\rho}_g^* + \mathrm{M}_l^* \, \bar{\rho}_l^* + \mathrm{C}^* + \frac{\mathrm{Fo}^+ \mathcal{A}_e^*}{\mathrm{Fo}_w \, R^* \, \mathcal{V}^*} \right) \frac{\mathrm{d}\bar{T}^*}{\mathrm{d}t^*} =$$

$$= - \frac{\mathrm{Fo}^+ \, \mathrm{Bi} \, \mathcal{A}_e^*}{\mathcal{V}^*} \left(\bar{T}^* - 1 \right) - \frac{\mathrm{Fo}^+ \, \mathrm{Bi}_{in} \, \mathcal{A}_i^*}{\mathcal{V}^*} \left(\bar{T}^* - T_{io}^* \right) + \mathrm{M}_l^* \, i_{sor}^* \, \frac{\mathrm{d}\bar{\rho}_l^*}{\mathrm{d}t^*} + \mathrm{M}_g^* \, \omega \, \frac{\mathrm{d}\bar{p}^*}{\mathrm{d}t^*} \quad (38)$$

Using the relation

$$\mathrm{Fo}_w \, R^* = \frac{\mathrm{Fo}^+ \, K_w}{\mathrm{C}_w^*}, \qquad \text{where} \qquad K_w = \frac{\mathcal{V}_w}{\mathcal{V}} \frac{L}{\delta_w} \approx \frac{\mathcal{A}_{ex} \, L}{\mathcal{V}} = K_{ex}, \tag{39}$$

recalling the dimensionless heat transfer coefficient defined by da Silva and Sphaier (2010)

$$\mathrm{H}^* = \frac{h \, \mathcal{A}_e \, t_f}{c_{p_g} \, \Delta m_{\max}} = \mathrm{Bi} \, \mathrm{Fo}^+ \, K_e, \qquad \text{where} \qquad K_e = \mathcal{A}_e \, L/\mathcal{V} = \mathcal{A}_e^*/\mathcal{V}^*, \tag{40}$$

and introducing a similar parameter for the inlet heat transfer coefficient:

$$\mathrm{H}_{in}^* = \frac{h_{in} \, \mathcal{A}_e \, t_f}{c_{p_g} \, \Delta m_{\max}} = \mathrm{Bi}_{in} \, \mathrm{Fo}^+ \, K_{in}, \qquad \text{where} \qquad K_{in} = \mathcal{A}_{in} \, L/\mathcal{V} = \mathcal{A}_{in}^*/\mathcal{V}^*, \tag{41}$$

then the lumped energy equation can be written as:

$$(\mathrm{M}_g^* \, \bar{\rho}_g^* + \mathrm{M}_l^* \, \bar{\rho}_l^* + \mathrm{C}^* + \mathrm{C}_w^*) \frac{\mathrm{d}\bar{T}^*}{\mathrm{d}t^*} = - \mathrm{H}^* \left(\bar{T}^* - 1 \right) - \mathrm{H}_{in}^* \left(\bar{T}^* - T_{io}^* \right) + \mathrm{M}_l^* \, i_{sor}^* \, \frac{\mathrm{d}\bar{\rho}_l^*}{\mathrm{d}t^*} + \mathrm{M}_g^* \, \omega \, \frac{\mathrm{d}\bar{p}^*}{\mathrm{d}t^*} \quad (42)$$

Finally the following dimensionless lumped formulation is obtained:

$$\mathrm{M}_g^* \, \frac{\mathrm{d}\bar{\rho}_g^*}{\mathrm{d}t^*} + \mathrm{M}_l^* \, \frac{\mathrm{d}\bar{\rho}_l^*}{\mathrm{d}t^*} = \dot{m}_{in}^*, \tag{43}$$

$$\left(\mathrm{M}_g^* \, \bar{\rho}_g^* + \mathrm{M}_l^* \, \bar{\rho}_l^* + \mathrm{C}_+^* \right) \frac{\mathrm{d}\bar{T}^*}{\mathrm{d}t^*} = \mathrm{H}^* \left(1 - \bar{T}^* \right) + \mathrm{H}_{in}^* \left(T_{io}^* - \bar{T}^* \right) + \mathrm{M}_g^* \, \omega \, \frac{\mathrm{d}\bar{p}^*}{\mathrm{d}t^*} + \mathrm{M}_l^* \, i_{sor}^* \, \frac{\mathrm{d}\bar{\rho}_l^*}{\mathrm{d}t^*}, \tag{44}$$

where C_+^* is the added contributions of the thermal capacity ratios, including the reservoir wall contribution:

$$\mathrm{C}_+^* = \mathrm{C}^* + \mathrm{C}_w^* = \mathrm{C}_{\min}^* + \mathrm{C}_s^* + \mathrm{C}_w^*. \tag{45}$$

5. TEST CASE

In order to compare the fully-lumped formulation with a model that takes into account local effects, a test-case problem, consisting of gas discharge at a constant mass flow rate (as usual for vehicular consumption applications) from a long cylindrical reservoir is considered. The resulting problem is a one-dimensional version of the multidimensional formulation being given by:

$$\mathrm{M}_g^* \, \frac{\partial \rho_g^*}{\partial t^*} + \mathrm{M}_l^* \, \frac{\partial \rho_l^*}{\partial t^*} = - \frac{1}{r^* + r_{in}^*} \frac{\partial}{\partial r^*} \left((r^* + r_{in}^*) \, j_{g,r}^* \right), \tag{46}$$

$$\left(\mathrm{M}_g^* \, \rho_g^* + c_p^* \, \mathrm{M}_l^* \, \rho_l^* + \mathrm{C}^*\right) \frac{\partial T^*}{\partial t^*} \, + \, j_{g,r}^* \, \frac{\partial T^*}{\partial r^*} \, =$$

$$= \, -\mathrm{Fo}^+ \, \frac{1}{r^* + r_{in}^*} \, \frac{\partial}{\partial r^*} \left((r^* + r_{in}^*) \, q_r^* \right) \, + \, \mathrm{M}_l^* \, i_{sor}^* \, \frac{\partial \rho_l^*}{\partial t^*} \, + \, \mathrm{M}_g^* \, \omega \, \frac{\partial p^*}{\partial t^*}, \quad (47)$$

where the heat and mass fluxes are given by:

$$j_{g,r}^* \, = \, -\mathrm{M}_g^* \, (\rho_g^* + \rho_{g,\min}^*) \, \sigma^* \, \frac{\partial p^*}{\partial r^*}, \tag{48}$$

$$q_r^* \, = \, -k_e^* \, \frac{\partial T^*}{\partial r^*}, \tag{49}$$

and r^* and r_{in}^* are defined as

$$r^* \, = \, \frac{r - r_{in}}{r_{ex} - r_{in}}, \tag{50}$$

$$r_{in}^* \, = \, \frac{r_{in}}{r_{ex} - r_{in}}. \tag{51}$$

The boundary conditions are given by:

$$j_{g,r}^* \, = \, 0, \qquad \text{at} \qquad r^* = 1, \tag{52}$$

$$-k_e^* \, \frac{\partial T^*}{\partial r^*} \, = \, \mathrm{Bi} \, (T^* - 1) + \frac{1}{\mathrm{Fo}_w \, R^*} \, \frac{\partial T^*}{\partial t^*}, \qquad \text{at} \qquad r^* = 1, \tag{53}$$

$$j_{g,r}^* \, = \, j_{in}^*, \qquad \text{at} \qquad r^* = 0, \tag{54}$$

$$k_e^* \, \frac{\partial T^*}{\partial r^*} \, = \, \mathrm{Bi}_{in}^+ \, (T^* - T_{io}^*), \qquad \text{at} \qquad r^* = 0, \tag{55}$$

in which, since a discharge operation is considered, $j_{in}^* < 0$. Also, an insulated inlet condition ($\mathrm{Bi}_{in}^+ = 0$) is considered, following other studies that simulate this discharge case (Barbosa Mota *et al.*, 1997b; Hirata *et al.*, 2009).

In the previously presented forms, the proposed formulations have four unknowns (ρ_g^*, ρ_l^*, T^* and p^*) and only two equations. Nevertheless, this is naturally overcome by introducing an equation of state for ρ_g and an adsorption equilibrium correlation (or adsorption isotherm) for ρ_l. An ideal gas equation of state is employed for expressing ρ_g in terms of temperature and pressure:

$$\rho_g \, = \, \rho_g(T, p) \, = \, \frac{p}{R \, T}, \tag{56}$$

and, for ρ_l, the Langmuir isotherm used in (Barbosa Mota *et al.*, 1997a,b; Hirata *et al.*, 2009) is adopted:

$$\frac{\rho_l}{\rho_b} \, = \, q_m \, \frac{b \, p}{1 + b \, p}, \tag{57}$$

in which

$$q_m = 5.592 \times 10^4 \, T^{-2.3}, \qquad b = 1.0863 \times 10^{-7} \exp(806/T). \tag{58}$$

6. RESULTS AND DISCUSSION

This section presents the results obtained from numerically solving the previously presented dimensionless formulations. Table 1 presents the data used in the simulations. The formulations are compared by evaluating differences between space-average temperature histories. Average pressure histories were also compared, but for the simulated case no noticeable difference was seen between the formulations, and the results need not be shown.
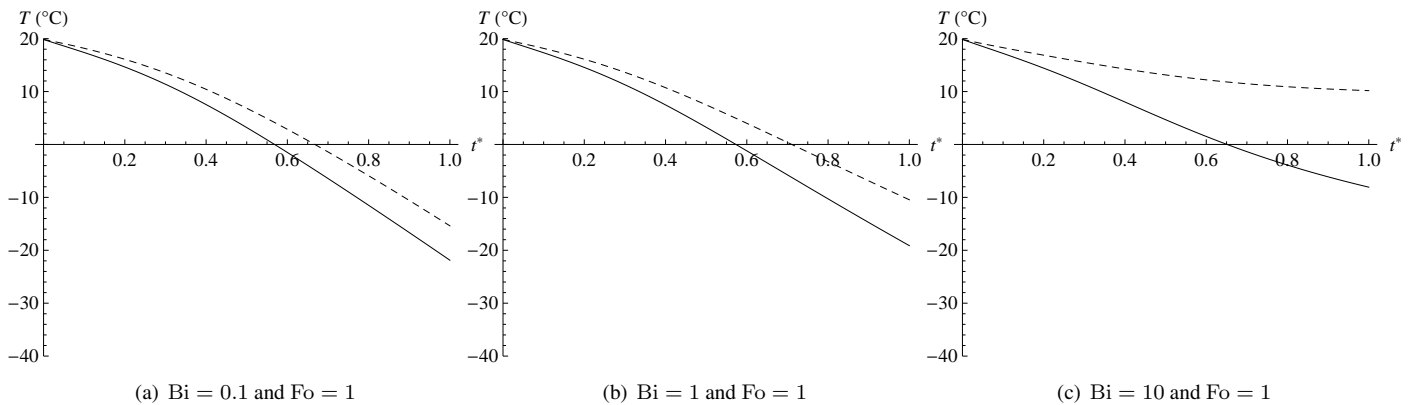
Figure 1 shows the evolution of the average temperature calculated with the one dimensional formulation (solid line) and the fully lumped formulation (dashed line), for Fo = 0.1 and different values of the Biot number. As can be seen, there is little variation among the three shown cases (Bi = 0.1, 1.0 and 10). Also, it is clear from these results that the lumped formulation underestimates the temperature decrease as gas is discharged.

As the Fourier number is increased to 1 (as displayed in figure 2) the case with larger Biot number shows a more significant variation when compared to Bi = 0.1 and Bi = 1. In addition it is seen that the lumped formulation approximates the one-dimensional one for the smaller Biot values.

For even higher values of the Fourier number, as seen in figure 3 (for Fo = 10) and in figure 4 (for Fo = 100), the results obtained with the different formulations become even closer. In fact, for Fo = 100 there is perfect graphical

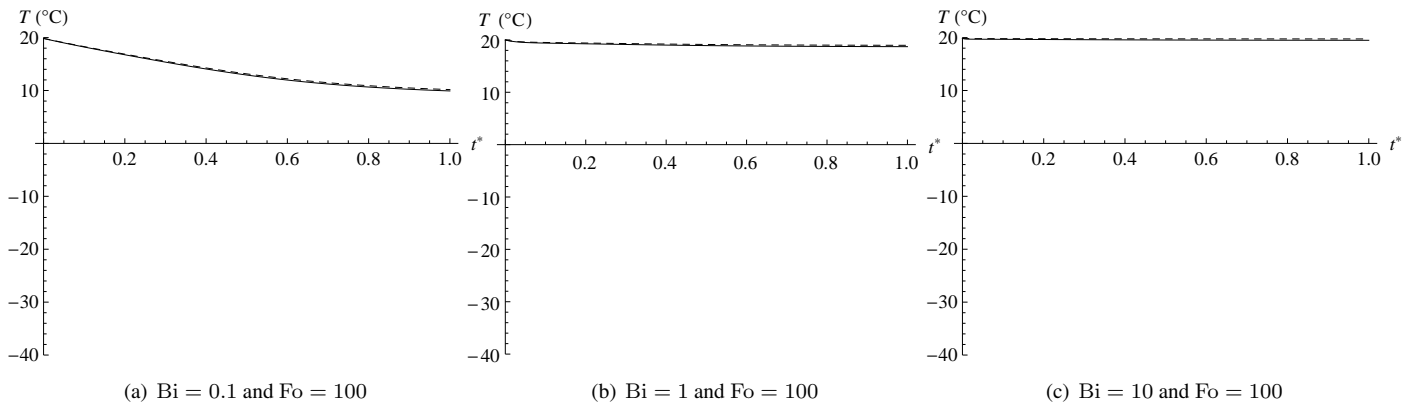Table 1. Input data used in the simulations

gas constant, R	518 J/(kg K)
ambient temperture, T_0	293.15 K
minimum pressure, $p_{\min}$	0.1 MPa
maximum pressure, $p_{\max}$	4 MPa
specific heat ratio, c_p^*	1
thermodynamic ratio, κ	1.3
conductivity coefficient, k_e^*	1
maximum adsorbed fraction, M_l^*	0.7
sorbent capacity ratio, C_s^*	2
minimum capacity ratio, $C_{\min}^*$	0.15
wall capacity ratio, C_w^*	5
inlet Biot number, Bi_{in}	0
dimensionless heat of sorption, i_{sor}^*	1.5

(a) Bi = 0.1 and Fo = 0.1   (b) Bi = 1 and Fo = 0.1   (c) Bi = 10 and Fo = 0.1
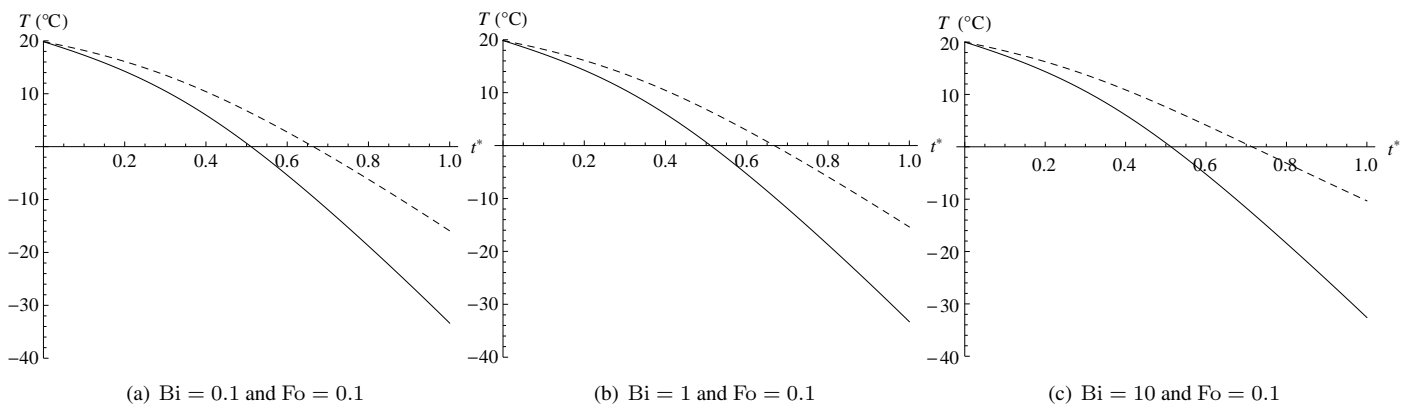
Figure 1. Comparisons between lumped and 1D formulation for Fo = 0.1.

(a) Bi = 0.1 and Fo = 1   (b) Bi = 1 and Fo = 1   (c) Bi = 10 and Fo = 1

Figure 2. Comparisons between lumped and 1D formulation for Fo = 1.

agreement between the results obtained with the lumped and one-dimensional formulations, regardless of the value of the Biot number. For all other cases where there is no perfect agreement between the lumped and the 1D formulations, if the Fourier number is held fixed, smaller Biot values lead to better agreement between the two formulations. This means that for slower processes, the lumped formulation is more accurate than for faster discharge operations. Also, if the heat transfer at the outer interface is increased the lumped formulation can also be used; however, the process speed will have a more strong impact on the accuracy of the lumped model, such that for very low processes, the lumped formulation could be used regardless of the convective heat transfer. Also, for fast process the lumped formulation cannot be employed accurately, even for a minor heat transfer coefficient at the interface.

As final comments, one should mention that, despite the different formulations, one clearly notices that as the Fourier

(a) Bi = 0.1 and Fo = 10   (b) Bi = 1 and Fo = 10   (c) Bi = 10 and Fo = 10
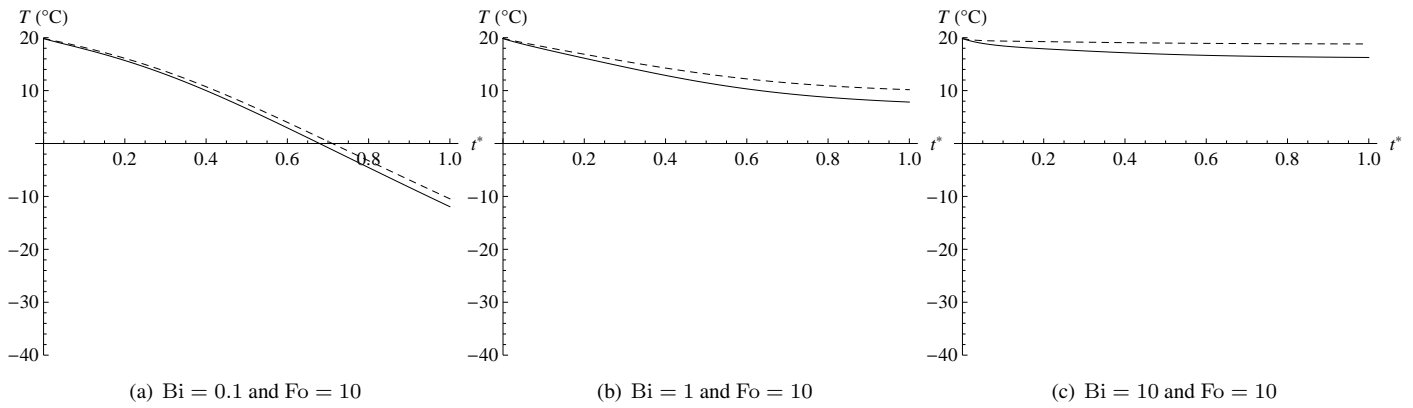
Figure 3. Comparisons between lumped and 1D formulation for Fo = 10.

(a) Bi = 0.1 and Fo = 100   (b) Bi = 1 and Fo = 100   (c) Bi = 10 and Fo = 100

Figure 4. Comparisons between lumped and 1D formulation for Fo = 100.

number and the Biot number are increased, the solution approaches an isothermal process. As a matter of fact, for Fo = 100 and Bi = 10 the solution is, apparently, totally isothermal. The closer to isothermal operation a gas discharge process is more gas can be recovered. This shows how large Fourier and Biot numbers can improve performance. In this context, by taking a final look at all figures, one sees that, since the lumped formulation tends to underestimate the cooling effect, it would end up overestimating the performance of a gas discharge operation if employed for inappropriate conditions.

7. CONCLUSIONS

This paper was aimed at determining the suitability of a lumped capacitance formulation for the simulation of adsorbed natural gas storage processes. The analysis was conducted by comparing the results of the lumped formulation with those calculated from a formulation with spatial dependence, which naturally considers heat and mass transfer as local phenomena. Before comparing the formulations it was shown that the lumped model can in fact be obtained from a multidimensional formulation by an averaging process followed by an approximation which considers small temperature and pressure gradients. A test-case problem of constant mass flow rate gas discharge operation was select for the comparisons, and a one-dimensional problem was employed for comparing results with the lumped formulation. The comparisons were carried out by varying values for dimensionless parameters and comparing the average temperature histories calculated from both formulations. Pressure histories were also calculated but theses were not shown since perfect agreement was found for all cases. The temperature histories calculated with both formulations were shown to present very different results for both cases under some situations. In general, the disparities were larger for smaller values of the Fourier number and higher values of the Biot number, indicating that the lumped formulation should not be employed for faster processes or if with a high convective heat transfer at the outer surface. It was also seen that the Fourier number had a more pronounced effect than the Biot number, such that for large Fourier numbers the Biot number has practically no effect on the disparity between the formulations. As a final remark one should mention that, despite the relevance of these findings, these results are still preliminary and further investigation should be carried out. For instance, other dimensionless parameters could be varied to verify if there are any other variables that can impact the applicability of a lumped formulation.

8. ACKNOWLEDGEMENTS

9. REFERENCES

Barbosa Mota, J.P., Rodrigues, A.E., Saatdjian, E. and Tondeur, D., 1997a. "Charge dynamics of methane adsorption storage system: intraparticle diffusional effects". *Adsorption*, Vol. 3, pp. 117–125.

Barbosa Mota, J.P., Rodrigues, A.E., Saatdjian, E. and Tondeur, D., 1997b. "Dynamics of natural gas adsorption storage system employing activated carbon". *Carbon*, Vol. 35, No. 9, pp. 1259–1270.

Bastos-Neto, M., Torres, A.E.B., Azevedo, D.C.S. and Jr., C.L.C., 2005. "A theoretical and experimental study of charge and discharge cycles in a storage vessel for adsorbed natural gas". *Adsorption*, Vol. 11, pp. 147–157.

Basumatary, R., Dutta, P., Prasad, M. and Srinivasan, K., 2005. "Thermal modeling of activated carbon based adsorptive natural gas storage system". *Carbon*, Vol. 43, No. 3, pp. 541–549.

da Silva, M.J.M. and Sphaier, L.A., 2010. "Dimensionless lumped formulation for performance assesment of adsorbed natural gas storage". *Applied Energy*, Vol. 87, No. 5, pp. 1572–1580.

Hirata, S.C., Couto, P., Larac, L.G. and Cotta, R.M., 2009. "Modeling and hybrid simulation of slow discharge process of adsorbed methane tanks". *International Journal of Thermal Sciences*, Vol. 48, No. 6, pp. 1176–1183.

Sacsa Diaz, R.P. and Sphaier, L.A., 2010. "Development of dimensionless groups for heat and mass transfer in adsorbed gas storage". *International Journal of Thermal Sciences*, Vol. submitted for publication.

Santos, J.C., Marcondes, F. and Gurgel, J.M., 2009. "Performance analysis of a new tank configuration applied to the natural gas storage systems by adsorption". *Applied Thermal Engineering*, Vol. 29, No. 11–12, pp. 2365–2372.

Vasiliev, L.L., Kanonchik, L., Mishkinis, D. and Rabetsky, M., 2000. "Adsorbed natural gas storage and transportation vessels". *International Journal of Thermal Sciences*, Vol. 39, pp. 1047–1055.

Walton, K.S. and LeVan, M.D., 2006. "Natural gas storage cycles: Influence of nonisothermal effects and heavy alkanes". *Adsorption*, Vol. 12, No. 3, pp. 227–235.

Zhou, Z.W., 1997. "Thermal analysis of slow discharge from a pressurized natural gas storage tank". *Applied Thermal Engineering*, Vol. 17, No. 11, pp. 1099–1110.

10. RESPONSIBILITY NOTICE

The authors are the only responsible for the printed material included in this paper.